Structural Chemistry of Chiral BINAP η^3-Allyl Complexes of Palladium(II). Multinuclear NMR and X-ray Diffraction Studies on Exo-Methylene Cyclopentene and β-Pinene Allyl Complexes

Paul S. Pregosin,* Heinz Rüegger, and Renzo Salzmann

Inorganic Chemistry, ETH-Zentrum, CH-8092 Zürich, Switzerland

Alberto Albinati* and Francesca Lianza

Chemical Pharmacy, University of Milan, I-20131 Milan, Italy

Roland W. Kunz

Organic Chemistry, University of Zürich, CH-8057 Zürich, Switzerland

Received July 1, 1994[⊗]

X-ray structural results for the *S*-BINAP pinene allyl compound [Pd(η^3-$C_{10}H_{15}$)(*S*-BINAP)]CF_3SO_3 (**1**) and the *R*-BINAP, exo-methylene cyclopentene allyl complex [Pd(η^3-C_6H_9)(*R*-BINAP)]CF_3SO_3 (**2**) together with multidimensional ^1H, ^{13}C, and ^{31}P NMR results for these and the new chiral allyl complex [Pd(η^3-C_6H_9)(*S,S*-CHIRAPHOS)]CF_3SO_3 (**3**) are presented. The results are interpreted in terms of differences in the chiral pockets between BINAP and *S,S*-CHIRAPHOS, i.e. the former has a phenyl array with more pronounced axial and equatorial character. The equatorial phenyl groups are suggested to intrude more into the sphere of the allyl ligand than do the axial phenyl groups. The differences in populations between the diastereomers for **2**, ca. 8:1, and for **3**, ca. 6:4, are explained. Several new empirical NMR tools, based on NOEs, are suggested to help in assigning the different coordinated faces of the η^3-C_6H_9 ligand. X-ray data for **1**, ortho rhombic, space group $P2_12_12_1$, $a = 11.762(1)$ Å, $b = 18.690(9)$ Å, $c = 21.240(3)$ Å, $V = 4669(2)$ Å^3; for **2**, monoclinic, space group $P2_1$, $a = 10.786(3)$ Å, $b = 11.250(5)$ Å, $c = 20.154(5)$ Å, $\beta = 101.72(2)°$, $V = 2395(1)$ Å^3.

Introduction

Organic synthesis with palladium,[1] and specifically catalytic allylation,[2] remains a reaction of considerable synthetic interest. If the allylation is carried out in the presence of a chiral auxiliary such as a chelating diphosphine, the organic products which result often reveal substantial-to-excellent enantiomeric excesses.[3] In recent times the nature of the chiral auxiliary has been altered to include chelating nitrogen ligands, with excellent results.[4]

In previous studies in palladium chemistry[5-11] we have demonstrated that ^1H NOE spectroscopy can be used to determine subtle and gross structural molecular features in organometallic complexes of Pd(II). Specifically, we have suggested that the *ortho* protons of phenyl groups attached to the P atoms may be used[5-7,10,11] as "reporters" to define aspects of the 3-D structure of chiral Pd–allyl catalyst precursors.

We report here two new X-ray structural results for the *S*-BINAP β-pinene allyl compound [Pd(η^3-$C_{10}H_{15}$)(*S*-BINAP)]CF_3SO_3 (**1**) and the *R*-BINAP, exo-methylene cyclopentene allyl complex [Pd(η^3-C_6H_9)(*R*-BINAP)]CF_3SO_3 (**2**) together with an NMR comparison of **2** with the new chiral allyl complex [Pd(η^3-C_6H_9)(*S,S*-CHIRAPHOS)]CF_3SO_3 (**3**). In our discussion we emphasize differences in the chiral pockets, e.g. between **2** and **3** as well as between **1** and its previously reported[5] *R*(+) analog **4** in addition to the ways in which the two allyl ligands coordinate as a function of the chiral phosphine.

[⊗] Abstract published in *Advance ACS Abstracts,* October 15, 1994.

(1) Trost, B. M. *Chemotracts: Org. Chem.* **1988**, *1*, 415. Trost, B. M. *Tetrahedron* **1977**, *33*, 2625. Pearson, A. J. *Metallo-Organic Chemistry*; John Wiley and Sons: New York, 1985. Stary, I.; Kocovsky, P. *J. Am. Chem. Soc.* **1989**, *111*, 4981.

(2) Consiglio, G.; Waymouth, R. M. *Chem. Rev.* **1989**, *89*, 257. Consiglio, G.; Indolese, A. *Organometallics* **1991**, *10*, 3425. Sawamura, M.; Ito, Y.; *J. Am. Chem. Soc.* **1992**, *114*, 2586.

(3) Yamamoto, K.; Deguchi, R.; Ogimura, Y.; Tsuji, J. *Chem. Lett.* **1954**, 1657. Mackenzie, P. B.; Whelan, J.; Bosnich, B. *J. Am. Chem. Soc.* **1985**, *107*, 2046. Auburn, P. R.; Mackenzie, P. B.; Bosnich, B. *J. Am. Chem. Soc.* **1985**, *107*, 2033. Hayashi, T.; Yamamoto, A. *Tetrahedron Lett.* **1988**, *29*, 669. Hayashi, T.; Yamamoto, A.; Ito, Y.; Nishioka, E.; Miura, H.; Yanagi, K. *J. Am. Chem. Soc.* **1989**, *111*, 6301. Sawamura, M.; Nagata, H.; Sakamoto, H.; Ito, Y. *J. Am. Chem. Soc.* **1992**, *114*, 2586.

(4) Pfalz, A. *Acc. Chem. Res.* **1993**, *26*, 339. von Matt, P.; Pfaltz, A. *Angew. Chem., Int. Ed. Engl.* **1993**, *32*, 566. Togni, A. *Tetrahedron Asymmetry* **1991**, *2*, 683.

(5) Pregosin, P. S.; Rüegger, H.; Salzmann, R.; Albinati, A.; Lianza, F.; Kunz, R. W. *Organometallics* **1994**, *13*, 83.

(6) Rüegger, H.; Pregosin, P. S. *Magn. Reson. Chem.* **1994**, *32*, 297.

(7) Pregosin, P. S.; Salzmann, R. *Magn. Reson. Chem.* **1994**, *32*, 128.

(8) Albinati, A.; Kunz, R. W.; Ammann, C. J.; Pregosin, P. S. *Organometallics* **1991**, *10*, 1800.

(9) Albinati, A.; Ammann, C.; Pregosin, P. S.; Rüegger, H. *Organometallics* **1990**, *9*, 1826.

(10) Ammann, C. J.; Pregosin, P. S.; Rüegger, H.; Abinati, A.; Lianza, F.; Kunz, R. W. *J. Organomet. Chem.* **1992**, *423*, 415.

(11) Rüegger, H.; Kunz, R. W.; Ammann, C. J.; Pregosin, P. S. *Magn. Reson. Chem.* **1992**, *29*, 197.

0276-7333/94/2313-5040$04.50/0

Scheme 1

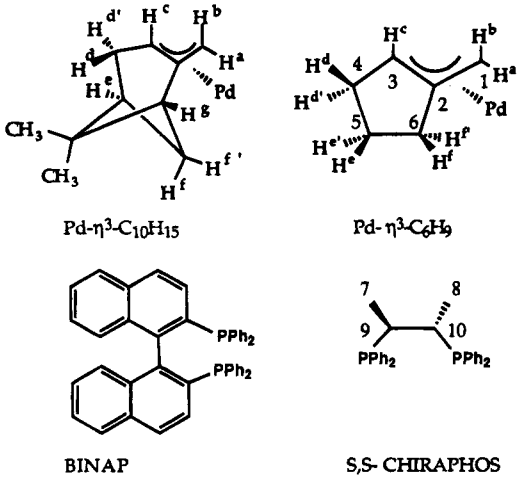

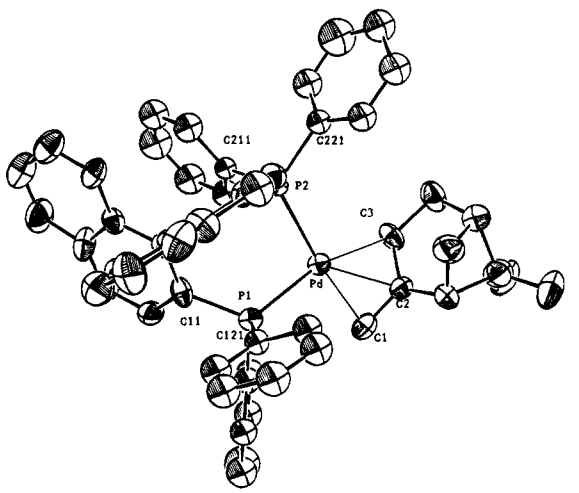

Figure 1. ORTEP plot for **1**.

Results and Discussion

The chloro-bridged allyl complexes were prepared using literature methods[12] and then reacted with the appropriate chelating phosphine ligand in the presence of $Ag(CF_3SO_3)$ to give the complexes **1**–**3** in good yield. In Scheme 1 we show the two allyl ligands and the numbering system for the various protons and carbons.

X-ray Structures of 1 and 2. The two new structures will be discussed together. ORTEP plots for the two cations are given in Figures 1 and 2, and Figures 3 and 4 show partial ORTEP plots designed to help envision the chiral pocket of the BINAP. A list of selected bond lengths and bond angles can be found in Table 1, experimental parameters in Table 2, and positional parameters in Tables 3 and 4.

The immediate coordination spheres for both **1** and **2** consist of the palladium atom, two P atoms of the BINAP, and the three allyl carbons of the η^3-$C_{10}H_{15}$ and η^3-C_6H_9 ligands. In both structures the Pd–P bond pseudo-trans to the allyl methylene carbon, 2.328(4) and 2.332(2) Å, respectively, is slightly longer than the Pd–P bond pseudo-trans to the allyl methine carbon, 2.302(4) and 2.293(3) Å, respectively. The observed Pd–P bond lengths are in good agreement with the literature[5,13–17] for allyl–phosphine complexes of Pd(II).

(12) Trost, B. M.; Strege, P. E. *J. Am. Chem. Soc.* **1975**, *97*, 2534.

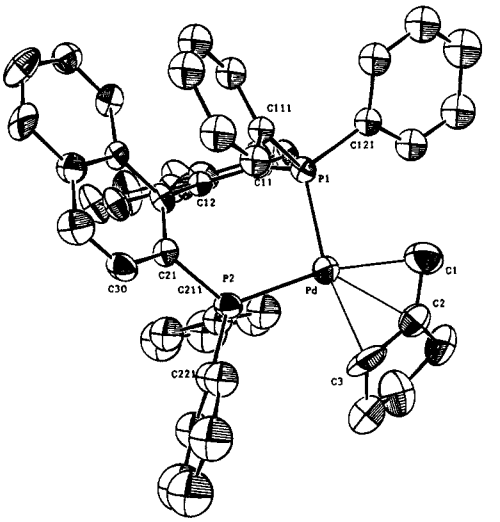

Figure 2. ORTEP plot for **2**.

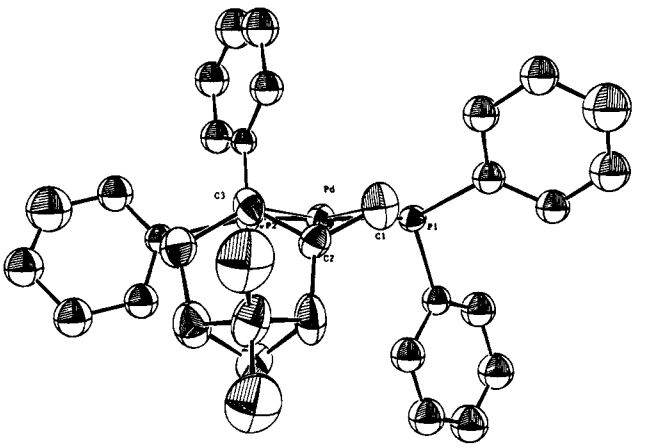

Figure 3. View of the chiral pocket of **1**.

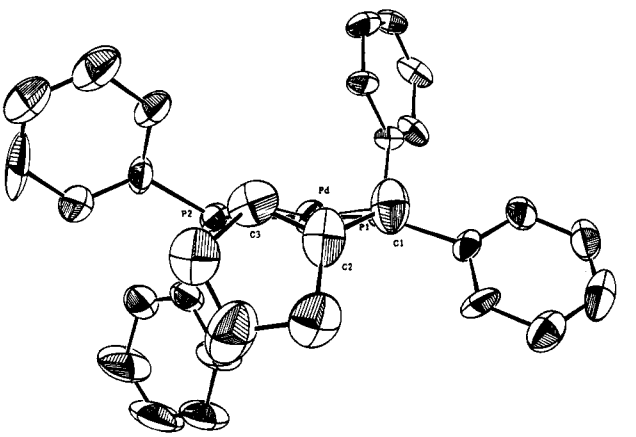

Figure 4. View of the chiral pocket of **2**.

The Pd–C(allyl) bond lengths have relatively large experimental uncertainties; however, it would appear that in both complexes these allyl carbons are ca. 2.2 Å from the metal, again in keeping with the literature.[5,13–17] The BINAP P–Pd–P angles are 94.4(1)° and 95.12(9)°

(13) Sprinz, J.; Kiefer, M.; Helmchen, G.; Reggelin, M.; Huttner, G.; Walter, O.; Zsolnai, L. *Tetrahedron Lett.* **1994**, *35*, 1523.
(14) Farrar, D. H.; Payne, N. C. *J. Am. Chem. Soc.* **1985**, *107*, 2054.
(15) Godleski, S. A.; Gundlach, K. B.; Ho, H. Y.; Keinen, E.; Frolow, F. *Organometallics* **1984**, *3*, 21.
(16) Knierzinger, A.; Schoholzer, P. *Helv. Chim. Acta* **1992**, *75*, 1211.
(17) Cesarotti, E.; Grassi, M.; Prati, L.; Demartin, F. *J. Chem. Soc., Dalton Trans.* **1991**, 2073.

Table 1. Selected List of Bond Angles (deg) and Bond Lengths (Å) for 1 and 2·CHCl$_3$

	1	2·CHCl$_3$
Pd−P(1)	2.328(4)	2.332(2)
Pd−P(2)	2.302(4)	2.293(3)
Pd−C(1)	2.15(2)	2.22(1)
Pd−C(2)	2.22(1)	2.21(1)
Pd−C(3)	2.25(1)	2.23(1)
C(1)−C(2)	1.39(2)	1.42(2)
C(2)−C(3)	1.42(2)	1.42(2)
P(1)−C(11)	1.83(1)	1.84(1)
P(1)−C(111)	1.81(1)	1.78(1)
P(1)−C(121)	1.88(1)	1.82(1)
P(2)−C(21)	1.85(1)	1.83(1)
P(2)−C(211)	1.84(1)	1.80(1)
P(2)−C(221)	1.83(1)	1.82(1)
P(1)−Pd−P(2)	94.4(1)	95.12(9)
P(1)−Pd−C(1)	168.8(5)	165.3(4)
P(2)−Pd−C(3)	160.8(4)	165.8(3)
P(1)−Pd−C(3)	103.9(4)	97.6(3)
P(2)−Pd−C(1)	95.0(5)	98.7(3)
C(1)−C(2)−C(3)	117(1)	123(1)
Pd−P(1)−C(11)	108.3(5)	114.2(3)
Pd−P(1)−C(111)	112.3(5)	115.7(4)
Pd−P(1)−C(121)	117.5(5)	109.5(4)
C(111)−P(1)−C(121)	102.6(7)	107.5(5)
C(211)−P(2)−C(221)	106.4(7)	106.2(5)

Table 2. Experimental Data for the X-ray Diffraction Studies of 1 and 2·CHCl$_3$

	1	2·CHCl$_3$
formula	$C_{55}H_{47}F_3O_3P_2PdS$	$C_{52}H_{42}Cl_3F_3O_3P_2PdS$
mol wt	1013.39	1078.68
crystal dim, mm	0.50 × 0.30 × 0.40	0.15 × 0.20 × 0.09
data collcn T, °C	23	23
cryst syst	orthorombic	monoclinic
space group	$P2_12_12_1$	$P2_1$
a, Å	11.762(1)	10.786(3)
b, Å	18.690(9)	11.250(5)
c, Å	21.240(3)	20.154(5)
β, deg		101.72(2)
V, Å^3	4669(2)	2395(1)
Z	4	2
ϱ(calcd), g cm^{-3}	1.442	1.496
μ, cm^{-1}	5.563	7.112
radiation (λ, Å)	Mo Kα (graphite monochromated) (0.71069)	
measd reflcns	$+h,+k,+l$	$\pm h,+k,+l$
θ range, deg	$2.5 < \theta < 25.0$	$2.5 < \theta < 25.0$
scan type	$\omega/2\theta$	$\omega/2\theta$
scan width, deg	$1.00 + 0.35 \tan\theta$	$1.10 + 0.35 \tan\theta$
max counting time, s	100	90
bkgd time, s	0.5 × scan time	0.5 × scan time
prescan rejectn limit	0.50 (2.00σ)	0.50 (2.00σ)
prescan accptnce limit	0.025 (40.00σ)	0.025 (40.00σ)
no. data colled	4548	6518
no. obs refctlns (n_o)	3202	5374
	$[\|F_o\|^2 > 3.0\sigma(\|F\|^2)]$	$[\|F_o\|^2 > 4.0\sigma(\|F\|^2)]$
transm coeff	0.9801−0.9975	0.8350−1.1902
decay corr		1.000−1.1517
no. params refined (n_v)	394	525
fudge factor f	0.065	0.070
max. param shift $\Delta p/\sigma$ (at convergence)	<0.15	<0.20
R^a	0.069	0.078
$R_w{}^b$	0.082	0.093
GOF^c	2.240	2.942

^{a} $R = \sum||F_o| - (1/k)|F_c||/\sum|F_o|$. ^{b} $R_w = [\sum w(|F_o| - (1/k)|F_c|)^2/\sum w|F_o|^2]^{1/2}$, where $w = [\sigma^2(F_o)]^{-1}$ and $\sigma(F_o) = [\sigma^2(F_o^2) + f^2(F_o^2)^2]^{1/2}/2F_o$. ^{c} GOF $= [\sum w(|F_o| - (1/k)|F_c|)^2/(n_o - n_v)]^{1/2}$.

for **1** and **2**, respectively, and lie at the upper end of the range observed[18,19] for BINAP transition metal complexes. Consequently, the PPh$_2$ groups are moved somewhat toward the allyl moieties. The corresponding value[5] for the $R(+)$ diastereomer [Pd(η^3-C$_{10}$H$_{15}$)(R-BINAP)]CF$_3$SO$_3$ (**4**) is 95.8(1)°. The angles between the

Table 3. Final Positional and Isotropic Equivalent Displacement Parameters for 1[a]

atom	x	y	z	B (Å^2)
Pd	0.06810(9)	0.04583(6)	0.89922(5)	2.39(2)
P1	0.0454(3)	−0.0764(2)	0.9163(2)	2.32(7)
P2	−0.1218(3)	0.0719(2)	0.9122(2)	2.42(6)
C1	0.115(2)	0.1526(9)	0.8712(9)	4.1(4)
C2	0.213(1)	0.1226(7)	0.8977(7)	2.9(3)
C3	0.252(1)	0.0568(9)	0.8719(7)	3.2(3)
C4	0.359(1)	0.027(1)	0.9028(9)	4.1(4)
C5	0.395(2)	0.071(1)	0.960(1)	4.7(4)
C6	0.401(1)	0.154(1)	0.942(1)	4.6(4)
C7	0.268(1)	0.150(1)	0.956(1)	4.6(4)
C8	0.289(2)	0.087(1)	1.0030(9)	4.4(4)
C9	0.461(2)	0.195(1)	0.994(1)	7.0(6)
C10	0.443(2)	0.173(1)	0.886(1)	7.1(6)
C11	−0.052(1)	−0.0886(8)	0.9825(6)	2.8(3)
C12	−0.170(1)	−0.0761(8)	0.9761(7)	2.8(3)
C13	−0.242(1)	−0.0741(9)	1.0312(7)	3.0(3)
C14	−0.358(1)	−0.0661(9)	1.0282(8)	3.7(3)
C15	−0.424(2)	−0.063(1)	1.0813(8)	4.3(4)
C16	−0.371(1)	−0.068(1)	1.1416(8)	4.9(4)
C17	−0.262(2)	−0.079(1)	1.1465(9)	5.0(4)
C18	−0.192(2)	−0.081(1)	1.0934(9)	4.4(4)
C19	−0.066(2)	−0.0948(9)	1.0963(7)	3.9(3)
C20	−0.006(1)	−0.0973(8)	1.0435(7)	3.1(3)
C21	−0.224(1)	0.0038(9)	0.8842(7)	3.1(3)
C22	−0.227(1)	−0.0646(8)	0.9141(6)	2.6(3)
C23	−0.294(1)	−0.1200(8)	0.8871(6)	2.8(3)
C24	−0.297(1)	−0.1886(9)	0.9157(9)	4.2(4)
C25	−0.353(2)	−0.244(1)	0.8853(9)	4.8(4)
C26	−0.414(2)	−0.230(1)	0.825(1)	5.6(5)
C27	−0.414(2)	−0.163(1)	0.801(1)	5.2(4)
C28	−0.357(1)	−0.104(1)	0.8297(8)	4.1(4)
C29	−0.352(1)	−0.0368(9)	0.8056(8)	3.8(3)
C30	−0.289(1)	0.0171(9)	0.8325(8)	3.5(3)
C111	−0.015(1)	−0.1215(8)	0.8488(6)	2.3(2)*
C1112	−0.019(1)	−0.087(1)	0.7935(8)	3.8(3)*
C113	−0.060(2)	−0.123(1)	0.7389(9)	5.0(4)*
C114	−0.099(2)	−0.189(1)	0.744(1)	5.7(5)*
C115	−0.095(2)	−0.227(1)	0.7983(9)	4.5(4)*
C116	−0.056(2)	−0.192(1)	0.8534(9)	4.1(3)*
C121	0.177(1)	−0.1306(8)	0.9322(7)	2.8(3)*
C122	0.207(2)	−0.181(1)	0.8913(9)	4.2(3)*
C123	0.302(2)	−0.223(1)	0.904(1)	6.8(5)*
C124	0.370(2)	−0.214(1)	0.954(1)	4.9(4)*
C125	0.340(2)	−0.155(1)	0.9967(9)	4.7(4)*
C126	0.241(1)	−0.116(1)	0.9851(8)	3.7(3)*
C211	−0.168(1)	0.1507(9)	0.8671(8)	3.3(3)*
C212	−0.136(1)	0.154(1)	0.8051(8)	3.9(3)*
C213	−0.167(2)	0.211(1)	0.7678(9)	4.2(4)*
C214	−0.233(2)	0.266(1)	0.796(1)	6.7(5)*
C215	−0.258(2)	0.263(1)	0.856(1)	4.8(4)*
C216	−0.228(1)	0.2072(9)	0.8932(8)	3.5(3)*
C221	−0.156(1)	0.0902(8)	0.9946(7)	2.8(3)*
C222	−0.066(2)	0.0974(9)	1.0375(8)	3.8(3)*
C223	−0.088(1)	0.114(1)	1.0985(9)	4.4(3)*
C224	−0.197(2)	0.120(1)	1.1198(9)	4.8(4)*
C225	−0.283(2)	0.115(1)	1.0779(9)	4.6(4)*
C226	−0.262(2)	0.098(1)	1.0143(9)	4.2(3)*
S	0.271	−0.065	1.187	6.6(1)*
O1	0.276	−0.081	1.125	9.8(6)*
O2	0.383	−0.039	1.206	21(2)*
O3	0.245	−0.130	1.221	34(3)*
C_f	0.164	0.005	1.210	36(6)*
F1	0.167	0.016	1.272	30(2)*
F2	0.187	0.067	1.179	26(2)*
F3	0.059	−0.018	1.193	32(2)*

[a] Starred atoms were refined isotropically. Anisotropically refined atoms are given in the form of the isotropic equivalent displacement parameter defined as $(4/3)[a^2\beta(1,1) + b^2\beta(2,2) + c^2\beta(3,3) + ab(\cos\gamma)\beta(1,2) + ac(\cos\beta)\beta(1,3) + bc(\cos\alpha)\beta(2,3)]$.

(18) Ashby, M. T.; Khan, M. A.; Halpern, J. *Organometallics* **1991**, *10*, 2011.

(19) (a) Mashima, K.; Kusano, K., Ohta, T., Noyori, R.; Takaya, H. *J. Chem. Soc., Chem. Commun.* **1989**, 466. (b) Ohta, T.; Takaya, H.; Noyori, R.; *Inorg. Chem.* **1988**, *27*, 566. (c) Toriumi, K.; Ito, T.; Takaya, H.; Souchi, T.; Noyori, R. *Acta Crystallogr.* **1982**, *B38*, 807.

Table 4. Final Positional and Isotropic Equivalent Displacement Parameters for 2·$CHCl_3$[a]

atom	x	y	z	B (Å^2)
Pd	0.76053(7)	0.689	0.25454(4)	2.99(1)
P1	0.7878(2)	0.7164(2)	0.1457(1)	2.23(5)
P2	0.9754(2)	0.7008(3)	0.3037(1)	2.84(5)
C1	0.554(1)	0.654(2)	0.2325(7)	5.4(4)
C2	0.591(1)	0.692(2)	0.3006(6)	5.2(3)
C3	0.691(1)	0.638(1)	0.3475(6)	4.9(3)
C4	0.714(1)	0.710(2)	0.4085(7)	6.2(4)
C5	0.663(2)	0.829(2)	0.387(1)	8.2(5)
C6	0.556(1)	0.811(2)	0.3277(8)	6.3(4)
C11	0.907(1)	0.8315(9)	0.1431(5)	2.3(2)
C12	1.034(1)	0.8136(8)	0.1686(5)	2.0(2)
C13	1.121(1)	0.9143(9)	0.1746(5)	2.6(2)
C14	1.252(1)	0.903(1)	0.1994(6)	3.5(3)
C15	1.330(1)	0.998(1)	0.2004(8)	5.2(3)
C16	1.282(1)	1.112(1)	0.1817(9)	5.3(3)
C17	1.158(1)	1.127(1)	0.1595(8)	5.2(3)
C18	1.073(1)	1.028(1)	0.1543(6)	3.4(3)
C19	0.941(1)	1.041(1)	0.1276(7)	3.6(3)
C20	0.861(1)	0.947(1)	0.1238(6)	3.2(2)
C21	1.081(1)	0.6401(9)	0.2509(5)	2.4(2)
C22	1.0904(8)	0.695(1)	0.1906(4)	2.3(2)
C23	1.1620(9)	0.6391(9)	0.1481(5)	2.4(2)
C24	1.1798(8)	0.690(1)	0.0857(5)	2.8(2)
C25	1.245(1)	0.634(1)	0.0455(6)	3.7(3)
C26	1.306(1)	0.524(1)	0.0651(7)	4.4(3)
C27	1.299(1)	0.477(1)	0.1245(7)	4.2(3)
C28	1.226(1)	0.530(1)	0.1683(6)	3.2(2)
C29	1.214(1)	0.479(1)	0.2319(6)	4.1(3)
C30	1.146(1)	0.531(1)	0.2702(6)	3.3(2)
C111	0.8417(9)	0.5838(9)	0.1100(5)	2.4(2)
C112	0.890(1)	0.582(1)	0.0526(5)	3.4(2)
C113	0.933(1)	0.475(1)	0.0293(6)	4.1(3)
C114	0.933(1)	0.376(1)	0.0648(6)	4.3(3)
C115	0.886(1)	0.376(1)	0.1249(7)	4.2(3)
C116	0.840(1)	0.479(1)	0.1465(6)	3.2(2)
C121	0.648(1)	0.766(1)	0.0851(5)	2.9(2)
C122	0.572(1)	0.853(1)	0.1038(7)	4.0(3)
C123	0.468(1)	0.899(1)	0.0599(8)	4.8(3)
C124	0.439(1)	0.852(1)	−0.0081(8)	5.8(3)
C125	0.511(1)	0.767(1)	−0.0264(7)	4.9(3)
C126	0.614(1)	0.720(1)	0.0191(6)	3.8(3)
C211	1.035(1)	0.847(1)	0.3244(6)	3.6(3)
C212	1.159(2)	0.869(1)	0.3475(7)	4.9(3)
C213	1.206(2)	0.991(1)	0.360(1)	7.8(5)
C214	1.118(2)	1.079(1)	0.346(1)	8.5(6)
C215	0.996(2)	1.060(1)	0.321(1)	7.1(5)
C216	0.952(1)	0.943(1)	0.3119(7)	5.1(3)
C221	1.008(1)	0.613(1)	0.3815(5)	3.4(2)
C222	1.068(1)	0.656(1)	0.4427(6)	4.8(3)
C223	1.086(2)	0.581(2)	0.5006(7)	8.1(5)
C224	1.040(2)	0.470(2)	0.4961(9)	7.3(5)
C225	0.975(2)	0.424(1)	0.4344(8)	6.3(4)
C226	0.960(1)	0.497(1)	0.3770(6)	4.0(3)
C_s	1.542(4)	0.939(4)	0.580(2)	15(1)*
Cl1	1.659(1)	0.836(1)	0.5814(6)	16.8(3)*
Cl2	1.405(1)	0.902(1)	0.5160(7)	17.7(4)*
Cl3	1.595(2)	1.066(2)	0.567(1)	23.9(6)*
S	0.6401(7)	1.2712(7)	0.2552(4)	10.1(2)*
O1	0.563(2)	1.274(2)	0.194(1)	12.7(5)*
O2	0.769(2)	1.298(2)	0.2621(9)	12.0(6)*
O3	0.566(6)	1.368(6)	0.270(3)	24(2)*
C_f	0.618(3)	1.186(4)	0.320(2)	15(1)*
F1	0.497(2)	1.161(2)	0.3194(8)	13.5(5)*
F2	0.685(2)	1.187(3)	0.374(1)	19.5(7)*
F3	0.6766(9)	1.0862(8)	0.3029(5)	6.9(2)*

[a] Starred atoms were refined isotropically. Anisotropically refined atoms are given in the form of the isotropic equivalent displacement parameter defined as $(4/3)[a^2\beta(1,1) + b^2\beta(2,2) + c^2\beta(3,3) + ab(\cos\gamma)\beta(1,2) + ac(\cos\beta)\beta(1,3) + bc(\cos\alpha)\beta(2,3)]$.

planes made by the three allyl carbons and the P−Pd−P coordination planes are 121(1)° and 122(1)° for **1** and **2**, respectively, with the C(2)−C(7) and C(2)−C(6) vectors pointing away from the Pd atom. In both **1** and **2** there is no substantial rotation of the allyl moiety,

Scheme 2. Fragments Reflecting the Differences in the Chiral Pockets between the *S* and *R* Diastereomers of [Pd(η^3-$C_{10}H_{15}$)(BINAP)]CF_3SO_3

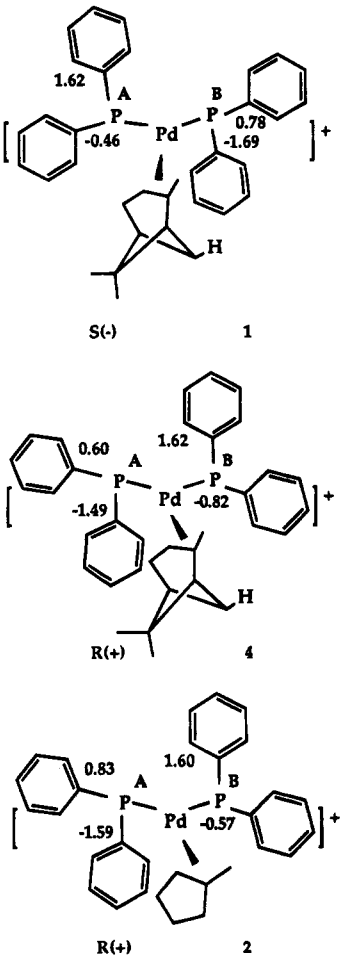

i.e., both terminal allyl carbons are ca. 0.2 Å from the P−Pd−P planes. This was not the case in the X-ray structure for the *R*-BINAP complex **4**. For **2** the solid-state structure corresponds to the structure of the major isomer in solution (the exo-methylene cyclopentene ligand is prochiral, so coordination affords diastereomers). The pseudo-trans angles P−Pd−C(allyl) fall in the range 161−169°.

Scheme 2 shows the displacements, in Å, of the ipso carbons of the phenyl substituents relative to the P−Pd−P coordination plane, for the two diastereomeric pinene complexes **1** and **4**. The view is from behind the organic allyl ligand and the naphthyl fragments have been omitted for clarity. In both cations the distances are consistent with pseudo-axial and pseudo-equatorial phenyl groups. If one ignores the signs of the numbers and compares the "left" and "right" distances, i.e., the values closest to the allyl methine, C(3), and the values closest to the allyl methylene, C(1), one finds that there are >0.1 Å differences on the left and <0.1 Å differences on the right, i.e., 1.62 vs −1.49 (Δ_{axial} = 0.13 Å) and −0.46 vs 0.60 (Δ_{equat} = 0.14 Å) for the ipso carbons close to C(3) and −1.69 vs 1.62 (Δ_{axial} = 0.07 Å) and 0.78 vs −0.82 (Δ_{equat} = 0.04 Å) for the ipso carbons close to C(1). Obviously the chiral pocket is somewhat different as a function of the interplay between the organic and BINAP chiralities. It seems likely that a "normal" distance for an axial ipso carbon would be ca. 1.6 Å and that the 1.49 Å value in **4** results from allyl hydrocar-

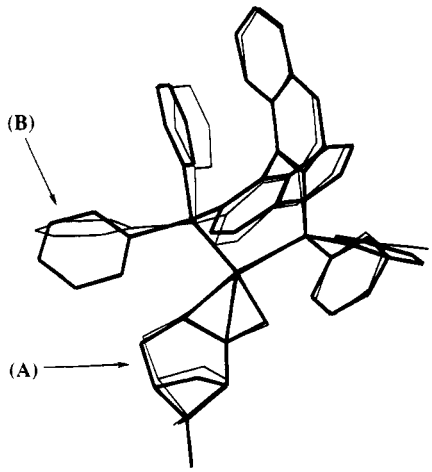

Figure 5. Comparison of the X-ray structure (bold) for **1** with the corresponding calculated structure. Note that the difference at the equatorial phenyl ring of P^A (B) is marked but that the agreement at the pinene allyl ligand (A) is good.

bon–phenyl ring repulsions. Further, we assume that a "normal" distance for an equatorial ipso carbon might be ca. 0.6–0.8 Å, so that, again, the 0.46 Å value in **1** arises from allyl hydrocarbon–phenyl repulsions. Such aliphatic hydrocarbon–phenyl repulsions are also consistent with the observed allyl rotation in the *R*(+) diastereomer **4** (C(1) is 0.61 Å and C(3) 0.17 Å above the plane[5]). It is worth noting that the pinene allyl ligand is not necessarily a typical allyl, in that it brings $H^{f'}$ (the proton indicated in Scheme 2), a seemingly innocent proton, relatively close to the axial phenyl group as witnessed by NOEs from this proton to the *ortho* protons of the axial phenyl group.

It is also interesting to compare **2** and **4**, both *R*(+) BINAP complexes, with respect to the positions of the BINAP ipso carbons of the phenyl substituents, and this is also given in Scheme 2. (a) There is no marked allyl rotation in **2** since C(1) is 0.19 Å and C(3) 0.24 Å above the plane. These values are similar to those noted above for **1**. (b) The two axial ipso carbons, C(111) and C(211) in **2**, are both 1.6 Å from the coordination plane and (c) the two equatorial ipso carbons, C(121) and C(221) at 0.83 Å and −0.57 Å, are both further away than the 0.46 Å distance for **1**, noted above and in Scheme 2. The η^3-C_6H_9 ligand is smaller than the η^3-$C_{10}H_{15}$ and perhaps this is the reason for the difference in these chiral pockets. These data suggest that structural conclusions based on relatively small allyl ligands such as the η^3-C_3H_5 anion may not reflect a general picture.

In review: for all three complexes, **1**, **2**, and **4**, the P–Pd–P angle is ca. 95°; the various Pd–P or Pd–C distances take on their normal lengths, and in one of these BINAP complexes, **4**, the allyl is rotated. There appears to be some difference between the chiral pockets of **1** and **4**.

MM2 vs X-ray. In an earlier report we predicted[10] the solution structure of **1** using MM2 methods. Consequently, it is interesting to see where the new solid-state result for **1** agrees and/or differs with our prediction and we show such a comparison in Figure 5. The overall agreement is reasonable with the two pinene allyls almost superimposed on one another (rms = 0.069 Å). The planes P–Pd–P and C–Pd–C (allyl terminal carbons) were predicted[10] and found to be almost coplanar; however, there are major differences between the predicted and observed BINAP skeletons (see Figure 5).

Table 5. ^{31}P NMR Data for [Pd(η^3-C_6H_9)(*S,S*-CHIRAPHOS)]CF_3SO_3

	δ^a	$^nJ(P_A,P_B)^b$
	R-BINAP	
major isomer		
P^A	22.5	50.8
P^B	22.9	
minor isomer		
P^A	27.7	48.7
P^B	23.2	
	S,S-CHIRAPHOS	
major isomer		
P^A	52.1	51.4
P^B	50.6	
minor isomer		
P^A	50.1	50.2
P^B	51.6	

[a] Chemical shifts in ppm, relative to external H_3PO_4 for $CDCl_3$ solutions at 297 K and at 202 MHz. [b] Coupling constants in hertz.

The most marked discrepancy arises at the equatorial phenyl ring of P^A (indicated by (B) in the figure), with the X-ray result showing this ring almost perpendicular to the P–Pd–P plane, whereas the MM2 calculation suggests this ring to be almost parallel to this plane. We know from our solution NMR studies that, at ambient temperature, there is *no* restricted rotation around the P^A_{eq}–C(ipso) bond. Further, we observe a moderate NOE between H^c and the *ortho* protons of P^A_{eq}, so that the X-ray result, which requires a ca. 4.7–4.8 Å separation between these two types of proton, cannot represent the solution structure at ambient temperature. However, our MM2 calculation makes the separation between these two spins to be ca. 2.3 Å, which is probably too short. Along the same lines, there is a calculated separation of ca. 2.5 Å from $H^{f'}$ (a bridgehead proton facing the palladium atom) to a binaphthyl proton, and we observe a relatively strong NOE between these spins. However, this differs from the ca. 3.4–3.5 Å distance between these two as given by the X-ray data. As we have noted previously,[10,11] there is no reason why the structures need to be identical. It is interesting that, again, the largest differences arise close to C-3, the substituted terminal allyl carbon.

NMR Spectroscopy. Table 5 gives ^{31}P NMR data and Tables 6 and 7 ^1H and ^{13}C NMR data for the new BINAP and CHIRAPHOS complexes **2** and **3**, respectively. The structures for the two exo-methylene cyclopentene diastereomers of [Pd(η^3-C_6H_9)(*R*-BINAP)]CF_3SO_3 (**2**) as well as for the two diastereomers of [Pd(η^3-C_6H_9)(*S,S*-CHIRAPHOS)]CF_3SO_3 (**3**) are shown in Scheme 3. It is normal to observe a mixture of diastereomers.[20]

Comparing the Two η^3-C_6H_9 Faces. We can distinguish between the major and minor diastereomeric forms in that we (a) first assign the allyl protons via NOE spectroscopy, (b) use a 2-D, ^{31}P,^1H correlation to assign the P atoms (via their correlations to the allyl protons), (c) use the same 2-D ^{31}P,^1H correlation to find and assign the *ortho* protons of the aromatic moieties

(20) Mackenzie, P. B.; Whelan, J.; Bosnich, B. *J. Am. Chem. Soc.* **1985**, *107*, 2046. Auburn, P. R.; Mackenzie, P. B.; Bosnich, B. *J. Am. Chem. Soc.* **1985**, *107*, 2033.

Table 6. ^{1}H and ^{13}C NMR Data for $[Pd(\eta^3\text{-}C_6H_9)(S,S\text{-CHIRAPHOS})]^+CF_3SO_3^-$

	δ^a				
	^{1}H	^{13}C	^1J(C,H)^b	^nJ(P,H)^b	^nJ(P,C)^b
	Major Isomer				
1a	4.29	62.5	163	6.1	30.2/3.3
1b	2.92		158	10.1	30.2/3.3
2		141.1			5.9/5.9
3c	4.23	91.0	164	9.8	29.8/4.5
4d	2.15	32.0	132		
4d′	1.51		140		
5e	1.55	25.0	138		
5e′	0.57		130		
6f	2.42	35.6	129		
6f′	1.87		138		
7g	1.12	13.5	132	12.2	15.4/5.3
8h	1.20	13.8	131	12.0	15.9/4.7
9i	2.32	34.5	136		29.1/16.4
10k	2.48	38.0	134		29.9/17.5
ortho-protons, carbons					
P^A_{ax}	7.59	131.5	164		10.8
P^A_{eq}	7.45	130.9	168		9.9
P^B_{ax}	7.35	134.8	171	7.1	13.9
P^B_{eq}	7.54	131.4	164		10.7
	Minor Isomer				
1a	4.06	62.7	163	4.0	
1b	3.15		159	10.0	
2		141.5			6.0/6.0
3c	4.15	92.3	164	9.3	30.2/5.2
4d	2.30	32.9	128		
4d′	1.97		136		
5e	1.76	24.7	138		
5e′	1.14		129		
6f	2.49	35.5	125		
6f′	1.91		139		
7g	1.16	14.2	131	11.8	15.8/4.8
8h	1.14	13.9	131	11.5	
9i	2.58	36.5	133		29.7/16.6
10k	2.42	38.5	136		30.1/17.1
ortho-protons, carbons					
P^A_{ax}	7.34	134.8	161		
P^A_{eq}	7.68	131.4	163		
P^B_{ax}	7.46	129.0	172		
P^B_{eq}	7.60	129.7	162		

[a] Chemical shifts in ppm, relative to TMS for $CDCl_3$ solutions at 297 K and at 500 and 126 MHz, for ^{1}H and ^{13}C, respectively. [b] Coupling constants in hertz.

(there are three types for each P atom, with the naphthyl proton having the simplest spin system), Figure 6, and (d) use selective NOEs from these *ortho* PPh_2 protons to the allyl protons to assign the structure and to differentiate the coordinated faces of the two diastereomers.

Occasionally point (c) can be non trivial and for BINAP complexes we have found that the *binaphthyl* proton *ortho* to the P atom shows a selective moderate NOE to the *ortho* protons of the pseudo-equatorial phenyl ring (see Figure 7), and this can be a useful extra assignment tool.

Point (d), assigning the diasteromers for the CHIRAPHOS complex **3**, is illustrated in Figure 8, in which we show that a syn proton, H^a, can reveal *two* strong NOEs to the PPh_2 *ortho* protons in the major isomer {one ring axial and one ring equatorial are both proximate to H^a; *S* configuration at C(3)}, but only one NOE to a PPh_2 *ortho* proton in the minor isomer {equatorial ring; *R* configuration at C(3)}. On the basis of our NOE results for **1**−**4** as well as on previously studied complexes, we find that the equatorial phenyls, rather than the axial phenyls, come closest to the organic allyl.

Table 7. ^{1}H and ^{13}C NMR Data for $[Pd(\eta^3\text{-}C_6H_9)(R\text{-BINAP})]^+CF_3SO_3^-$

	δ^a				
	^{1}H	^{13}C	^1J(C,H)^b	^nJ(P,H)^b	^nJ(P,C)^b
	Major Isomer				
1a	3.33	70.3	164	4.7	31.4
1b	3.96		160	9.2	
2		141.9			5.5/5.5
3c	4.22	97.3	168	10.5	28.6/5.8
4d	1.75	31.7	128		
4d′	0.90		129		
5e	1.82	25.0	125		
5e′	1.53		132		
6f	2.52	35.4	141		
6f′	2.29		135		
ortho-protons, carbons					
P^A_{ax}	7.09	134.4	162	11.1	
P^A_{eq}	7.73	135.0	164	10.0	
P^B_{ax}	7.32	135.2	164	11.5	14.2
P^B_{eq}	7.51	133.8	163		
naphthyl-protons, carbons					
ortho to P^A	7.78	126.0	166	9.0	9.3
ortho to P^B	7.25	126.3	165	9.0	9.2
	Minor Isomer				
1a	3.93	67.9	163	6.1	28.5
1b	3.14		162	10.2	
2		141.4			
3c	5.13	92.8	167	10.5	
4d	2.14	32.2			
4d′	1.69				
5e	1.89	25.3			
5e′	1.30				
6f	2.53	35.4			
6f′	2.10				
ortho-protons, carbons					
P^A_{ax}	7.19[c]	134.5			
P^A_{eq}	7.73[c]	133.0			
P^B_{ax}	6.84[c]	134.2			
P^B_{eq}	7.66[c]	133.3			
naphthyl-protons, carbons					
ortho to P^A	7.60[c]	127.0	167		
ortho to P^B	7.17[c]				

[a] Chemical shifts in ppm, relative to TMS for $CDCl_3$ solutions at 297 K and at 500 and 126 MHz, for ^{1}H and ^{13}C, respectively. [b] Coupling constants in hertz. [c] From P−H correlation.

Scheme 3. Molecular Fragments for 2 and 3, Showing the Coordination of the η^3-C_6H_9 Ligand[a]

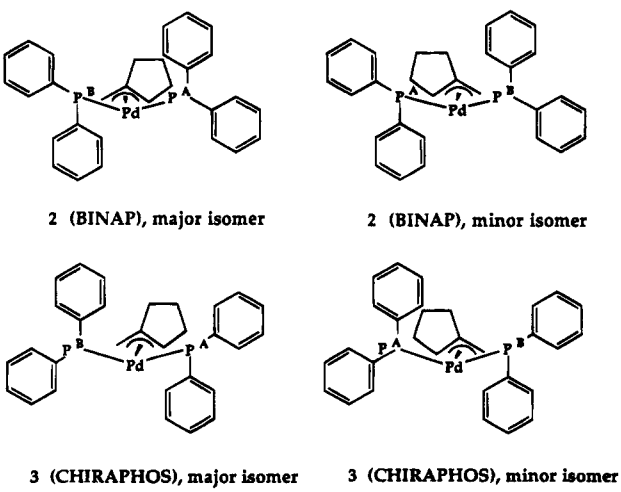

2 (BINAP), major isomer 2 (BINAP), minor isomer

3 (CHIRAPHOS), major isomer 3 (CHIRAPHOS), minor isomer

[a] The sketches do not reflect the actual chiral pocket for *S,S*-CHIRAPHOS, see text.

Comparing differences within one set of diastereomers with respect to their methylene and methine terminal allyl ^{13}C chemical shifts, C(1) and C(3), respectively, we find that the separations in the chemical shifts between the diastereomers are modest, except for C(3) in **2**, 4.9

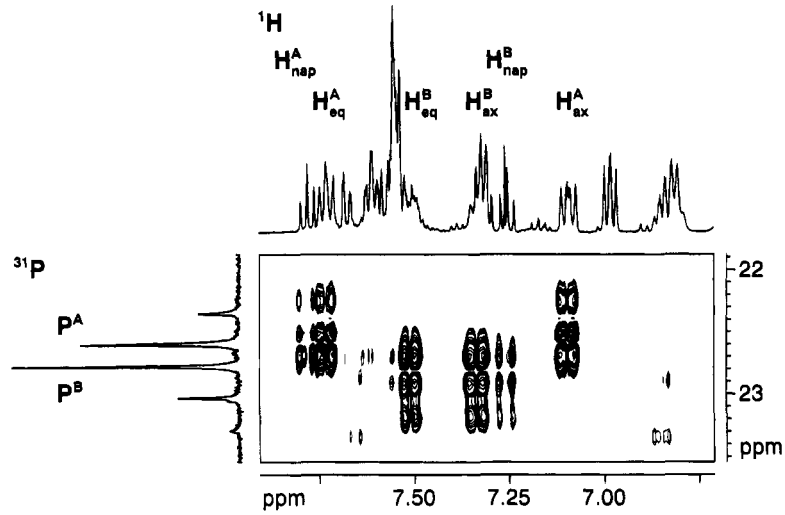

Figure 6. Section of the ^{31}P,^{1}H correlation showing the correlation of the individual ^{31}P spins of the major isomer of **2** to the six *ortho* protons (three for each P atom). The naphthyl proton has a much simpler spin system, so that the cross-peak do not appear as broad as for the corresponding protons of the PPh_2 groups ($CDCl_3$, 500 MHz).

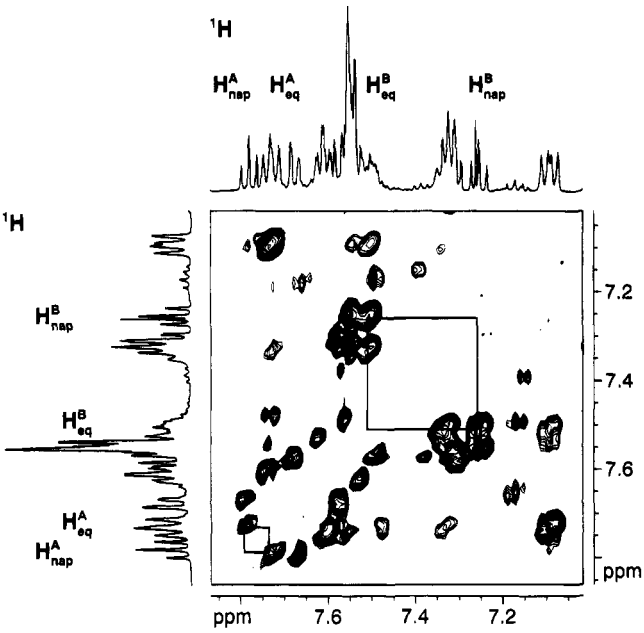

Figure 7. Section of the ^{1}H NOESY for **1** indicating the selective NOEs from the *ortho* naphthyl protons to the *ortho* equatorial PPh_2 protons via the solid lines, lower left and center ($CDCl_3$, 500 MHz). This helps in distinguishing axial and equatorial *ortho* PPh_2 protons. Note that the diagonal is omitted for clarity.

ppm. Consequently, we consider it likely that the source of the differentiation is steric in origin.

Comparison of BINAP with CHIRAPHOS. The relative amounts of the two diastereomeric isomers in **2** and **3** is dependent on the phosphine, with the ratio for BINAP = 8:1 and that for *S,S*-CHIRAPHOS = 6:4, as shown in Figure 9. Obviously the BINAP chelate ligand, with its larger P–Pd–P angle, affects the relative populations of the two diastereomers.

Comparing the two major diastereomers from the η^3-C_6H_9 compounds **2** and **3**, one observes that the ^{13}C chemical shift of C(1) with BINAP appears at δ = 70.3 ppm, whereas C(1) for *S,S*-CHIRAPHOS appears at δ = 62.5 ppm. The analogous values for C(3) are 97.3 and 91.0 ppm, respectively. We have found a similar trend for the allyl $^{13}CH_2$ signals in the η^3-$C_{10}H_{15}$ BINAP and *S,S*-CHIRAPHOS cations (74.5 and 72.9 ppm for the *R*- and *S*-BINAP complexes and 67.4 in the *S,S*-CHIRAPHOS complex). Since a high frequency ^{13}C allyl shift is usually associated with a stronger trans influence[21] (the *source* of the difference can be electronic and/or steric), we conclude that the BINAP seems somewhat more labilizing in the ground state than *S,S*-CHIRAPHOS. It is also interesting that the differences in the P^A (= trans to allyl CH_2) ^{31}P chemical shifts between the diastereomers, **3**, is much more pronounced with BINAP, 5.2 ppm, than with the *S,S*-CHIRAPHOS pair, **2**, 2.0 ppm.

On the Chiral Pocket. It would seem that, since we have an *R*-BINAP in **2** and an *S,S*-CHIRAPHOS in **3**, we cannot compare the two in terms of their chiral pockets. However, the major diastereomer in **2**, *R*(BINAP),*S*(allyl) gives identical NMR spectra as the *S*(BINAP),*R*(allyl) diastereomer. Since we have ample amounts of the two diastereomers in **3**, (*S,S*),*S*(allyl) = major component, and (*S,S*),*R*(allyl) = minor component, we can compare data from the major diastereomer of **2** with those from the minor diastereomer of **3**. One can do this for the ^{13}C chemical shifts of the terminal allyl carbons:

	BINAP	CHIRAPHOS
δ^{13}C(1)	70.3	62.7
δ^{13}C(3)	97.3	92.3

but it is more informative to look at analogous NOE contacts to the same allyl protons and specifically for H^c, the methine terminal allyl proton. For the BINAP H^c case, there are *three-to-four contacts* with a very strong interaction stemming from the *ortho* protons of the phenyl P^A_{eq}. There is also a moderately strong interaction with the *ortho* protons of the phenyl P^B_{ax}. For the CHIRAPHOS H^c proton, there is only *one* moderate contact, again arising from the *ortho* protons of the phenyl P^A_{eq}. An analogous comparison of NOEs for H^a and H^b reveals no special selectivity. We conclude that, for this comparison, the BINAP chiral pocket is much more intrusive where there is an allyl

(21) Åkermark, B.; Krakenberger, B.; Hansson, B.; Vitagliano, A. *Organometallics* **1987**, *6*, 620.

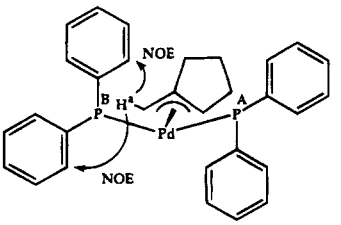

3 (CHIRAPHOS), major isomer

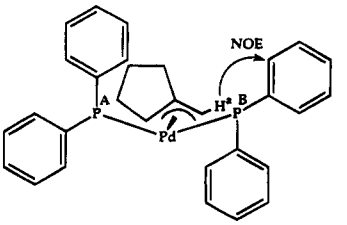

3 (CHIRAPHOS), minor isomer

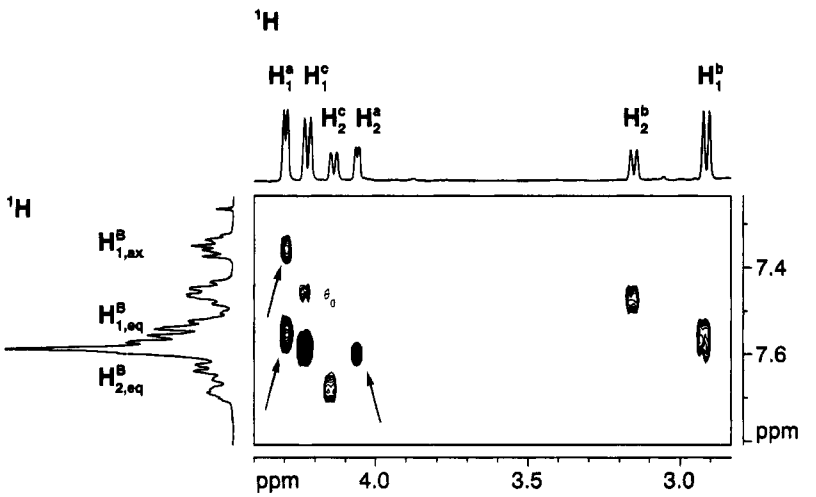

Figure 8. Section of the ^1H NOESY for **3** indicating the selective NOEs from the allyl protons to the *ortho* PPh_2 phenyl protons. Note that for H^a of the major isomer there are *two* such NOEs, whereas for H^a of the minor isomer there is only one, thereby helping to differentiate the two diastereomers ($CDCl_3$, 500 MHz).

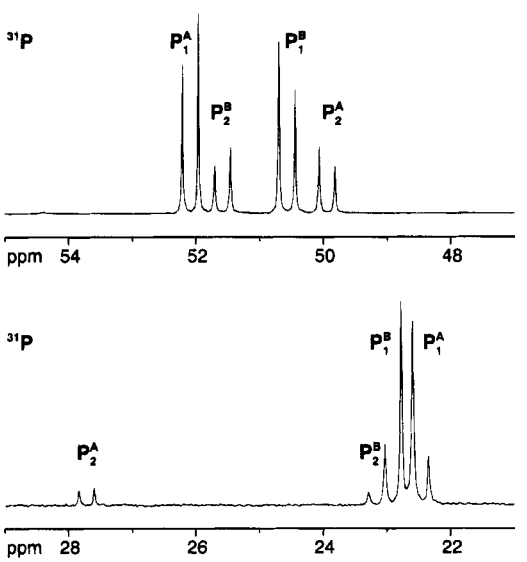

Figure 9. Conventional ^{31}P NMR spectra for **2** and **3**, showing the different amounts of the diastereomers within each ($CDCl_3$, 202 MHz).

fragment of some steric bulk, i.e., the substituents on C(3) interact more than those on the sterically modest C(1). Why is the CHIRAPHOS "H^c, P^A_{eq}" contact only moderate? We believe that this comes from the *lack* of pronounced axial or equatorial character for the four phenyl groups as described by us[7] and others previously.[22]

Conclusions. Taken together, the X-ray and NMR data point clearly to differences between **1** and **4** as well as between **2** and **3**. These differences arise as a consequence of the positioning of the PPh_2 phenyl groups with respect to the allyl ligand, i.e., they are a function of the chiral pocket. Both types of measurement reveal that the differences are most marked when there is substantial steric bulk in the organic ligand.

Experimental Section

The ligands *S,S*-CHIRAPHOS and *S*-BINAP were commercially available. The NMR spectra were obtained from $CDCl_3$ solutions using a Bruker AMX 500 spectrometer. Standard pulse sequences[23-25] were used for the NOESY, $^{13}C,^1H$, and $^{31}P,^1H$ spectra. NOESY spectra were measured using a 0.8 s mixing time. The chloro-bridged dimer was prepared according to the literature.[12]

Preparation of 2 and 3. The chloro-bridged dimer (0.025 mmol) and the chiral phosphine (0.05 mmol) were added to 5 mL of methanol and the suspension stirred for 10 min until a clear solution resulted. This was followed by addition of $Ag(CF_3SO_3)$ (0.055 mmol) and stirring for a further 10 min. The resulting suspension was filtered through Celite to remove AgCl, and the solvent was distilled. The resulting solid was dissolved in CH_2Cl_2 and the solution filtered through Celite. After removal of the CH_2Cl_2, the complexes were recyrstallized from $CHCl_3$/ether. The yield for **2** was 38 mg (82%) and for **3**, 24 mg (51%). Anal. Calcd for **2**: C, 63.60; H, 4.67. Found: C, 63.85; H, 4.30. Anal. Calcd for **3**: C, 55.09; H, 4.89. Found: C, 55.07; H, 4.75.

Crystallography. Crystals suitable for X-ray diffraction of **1**, and **2**·$CHCl_3$ were obtained by crystallization from

(22) Giovanetti, J. S.; Kelly, C. M.; Landis, C. R. *J. Am. Chem. Soc.* **1993**, *115*, 4040.

(23) Jeener, J.; Meier, B. H.; Bachmann, P.; Ernst, R. R. *J. Chem. Phys.* **1979**, *71*, 4545.

(24) Summers, M. F.; Marzilli, L. G.; Bax, A. *J. Am. Chem. Soc.* **1986**, *108*, 4285.

(25) Sklener, V.; Miyashiro, H.; Zon, G.; Miles, H. T.; Bax, A. *FEBS Lett.* **1986**, *208*, 94.

benzene/hexane (1:3) and $CHCl_3$/hexane/ether (3:4:1), respectively. Crystals of both compounds were mounted on glass fibers at a random orientation on an Enraf-Nonius CAD4 diffractometer for the unit cell and space group determinations and for the data collection (**2**·$CHCl_3$ was covered for protection with acrylic resin). Unit cell dimensions were obtained by least-squares fit of the 2θ values of 25 high-order reflections (in the interval $9.4° < \theta < 15.1°$ for **1** and $9.3° < \theta < 16.2°$ for **2**) using the CAD4 centering routines. Selected crystallographic and other relevant data are listed in Table 2.

Data were measured with variable scan speed to ensure constant statistical precision on the collected intensities. Three standard reflections were used to check the stability of the crystal and of the experimental conditions and measured every hour. The orientation of the crystal was checked by measuring three reflections every 300 measurements. Data have been corrected for Lorentz and polarization factors and for decay (compound **2**·$CHCl_3$) using the data reduction programs of the MOLEN[26] package. Empirical adsorption corrections were applied to both sets of data by using azimuthal (Ψ) scans of "high-χ" angle reflections (for **1** three reflections with $\chi > 86.7°$ and for **2**·$CHCl_3$ two reflections with $\chi > 88.2°$). The standard deviations on intensities were calculated in terms of statistics alone, while those on F_o were calculated as shown in Table 2.

The structures were solved by a combination of Patterson and Fourier methods and refined by full matrix least-squares[26] (the function minimized being $\Sigma[w(F_o - (1/k)F_o)^2]$).

Anisotropic displacement parameters were used for all atoms of the cation of compound **2**·$CHCl_3$ while for the cation of **1** the phenyl rings were treated isotropically, given the less favorable observations-to-parameters ratio.

As often found, the $CF_3SO_3^-$ counterions are highly disordered in both compounds; therefore models were constructed on the basis of the strongest peaks in the Fourier difference maps. In compound **1** only the isotropic displacement factors of the triflate were refined while for **2**·$CHCl_3$ both positional and thermal factors were refined.

The contribution of the hydrogen atoms in calculated positions (C−H = 0.95 Å, $B(H) = 1.3 \times B(C_{bonded})$ (Å^2)) was taken into account but not refined.

No extinction correction was found to be necessary. The scattering factors used, corrected for the real and imaginary parts of the anomalous dispersion,[27] were taken from ref 27.

The handedness of the structures were tested by refining both sets of coordinates. Those giving the significantly lower R_W factors were used.[28] All calculations were carried out using the Enraf-Nonius MOLEN package.[26]

Final atomic coordinates and isotropic equivalent displacement parameters for both compounds are given in Tables 3 and 4, respectively.

Acknowledgment. P.S.P. thanks the Swiss National Science Foundation and the ETHZ for support and Johnson Matthey, Reading, England, for the loan of palladium salts. A.A. thanks MURST for support.

Supplementary Material Available: For **1** and **2**, tables of calculated positional parameters for the hydrogen atoms (Tables S1 and S2) and anisotropic displacement parameters (Tables S3 and S4), an extended list of bond distances and bond angles (Tables S5 and S6), and full numbering schemes for both (Figures SF1 and SF2) (30 pages). Ordering information is given on any current masthead page.

OM940518+

(26) MOLEN: Molecular Structure Solution Procedure; Enraf Nonius, Delft, The Netherlands, 1990.

(27) *International Tables for X-ray Crystallography*; Kynoch Press: Birmingham, England, 1974; Vol. IV.

(28) Hamilton, W. C. *Acta Crystallogr.* **1965**, *13*, 502.